Endocrinology. First published ahead of print September 7, 2012 as doi:10.1210/en.2012-1303

Molecular Basis for Glucocorticoid Induction of the Krüppel-Like Factor 9 Gene in Hippocampal Neurons

Pia Bagamasbad, Tim Ziera, Steffen A. Borden, Ronald M. Bonett, Aaron M. Rozeboom, Audrey Seasholtz, and Robert J. Denver

Department of Molecular (P.B., R.J.D.), Cellular and Developmental Biology, University of Michigan, Ann Arbor, Michigan 48109-1048; Bayer Healthcare Pharmaceuticals (T.Z., S.A.B.), Research Laboratories, 13353 Berlin, Germany; Department of Biological Science (R.M.B.), University of Tulsa, Tulsa, Oklahoma 74104-3189; and Molecular and Behavioral Neuroscience Institute (A.M.R., A.S.) and Cellular and Molecular Biology Program (A.M.R.), University of Michigan, Ann Arbor, Michigan 48109-5720

Stress has complex effects on hippocampal structure and function, which consequently affects learning and memory. These effects are mediated in part by circulating glucocorticoids (GC) acting via the intracellular GC receptor (GR) and mineralocorticoid receptor (MR). Here, we investigated GC regulation of Krüppel-like factor 9 (KLF9), a transcription factor implicated in neuronal development and plasticity. Injection of corticosterone (CORT) in postnatal d 6 and 30 mice increased *Klf9* mRNA and heteronuclear RNA by 1 h in the hippocampal region. Treatment of the mouse hippocampal cell line HT-22 with CORT caused a time- and dose-dependent increase in *Klf9* mRNA. The CORT induction of *Klf9* was resistant to protein synthesis inhibition, suggesting that *Klf9* is a direct CORT-response gene. In support of this hypothesis, we identified two GR/MR response elements (GRE/MRE) located −6.1 and −5.3 kb relative to the transcription start site, and we verified their functionality by enhancer-reporter, gel shift, and chromatin immunoprecipitation assays. The −5.3-kb GRE/MRE is largely conserved across tetrapods, but conserved orthologs of the −6.1-kb GRE/MRE were only detected in therian mammals. GC treatment caused recruitment of the GR, histone hyperacetylation, and nucleosome removal at *Klf9* upstream regions. Our findings support a predominant role for GR, with a minor contribution of MR, in the direct regulation of *Klf9* acting via two GRE/MRE located in the 5′-flanking region of the gene. KLF9 may play a key role in GC actions on hippocampal development and plasticity. **(*Endocrinology* 153: 0000–0000, 2012)**

The hippocampus is an important target for the actions of circulating glucocorticoids (GC). GC actions on the hippocampus are complex: they may facilitate or impair hippocampal function by influencing cell survival, dendritic remodeling, and synaptic transmission (1, 2). The actions of GC are mediated in large part by two nuclear receptors that function as ligand-activated transcription factors, the mineralocorticoid receptor (MR) and the GC receptor (GR) (3); both are highly expressed in the mammalian hippocampus (4, 5). The MR and GR bind to DNA at hormone-response elements comprised of two hexanucleotide half-sites and they recruit coactivator or corepressor complexes that contain histone modifying enzymes (6, 7). The histone modifications promote an open or closed chromatin environment, thereby influencing the rate of transcription (8).

Stress hormones cause biochemical, physiological, and structural changes in neurons (9). Several direct transcriptional targets of the GR have been identified in hippocampal neurons (10–14), but the mechanisms by which GC influence neuronal structure and function are poorly understood. Earlier we found that the transcription factor Krüppel-like factor 9 (KLF9) is a direct thyroid hormone (TH) target gene that is strongly up-regulated during post-

ISSN Print 0013-7227 ISSN Online 1945-7170
Printed in U.S.A.

doi: 10.1210/en.2012-1303 Received March 17, 2012. Accepted August 8, 2012.

Abbreviations: AcH3, Acetylated H3; ALDO, aldosterone; ChIP, chromatin immunoprecipitation; CHX, cycloheximide; CMV, cytomegalovirus; CORT, corticosterone; DBD, DNA binding domain; DEX, dexamethasone; DNAse, deoxyribonuclease; FBS, fetal bovine serum; GC, glucocorticoid; GR, GC receptor; GRE, GC-response element; H3, histone 3; hGR, human GR; hnRNA, heteronuclear RNA; KLF9, Krüppel-like factor 9; MMTV, mouse mammary tumor virus; MR, mineralocorticoid receptor; MRE, mineralocorticoid-response element; PND, postnatal day; RTqPCR, reverse transcription quantitative PCR; RU486, mifepristone; SPR, spironolactone; TESS, Transcription Element Search System; TH, thyroid hormone; T_3RE, T_3-response element; TSS, transcription start site.

natal brain development (15, 16). The *Klf9* gene is expressed in several rodent tissues, but highest expression is seen in the hippocampus and cerebellum of the developing brain (17–19). *Klf9* expression was detected in the hippocampus at postnatal day (PND) 1, which increased through PND 5, at which time there was distinct expression in the pyramidal cell layer; strong expression in the cortical layer of the cerebellum was detected at PND 7 (19). Expression in the hippocampus peaked at PND 15, remained elevated through PND 30, but then declined in the adult to levels seen at PND5 (16, 19, 20). The developmental increase in *Klf9* expression parallels the postnatal rise in plasma TH seen in rodents (15, 16, 19–21), which supports findings that KLF9 functions as a key intermediary in TH actions on neuronal structure and function (15, 22).

KLF9 plays a role in neuronal maturation and morphology, and hippocampal and cerebellar function. KLF9-deficient mice exhibited reduced dendritic arborization of cerebellar Purkinje cells (19), delayed neuronal maturation and reduced neurogenesis-dependent long-term potentiation in the dentate gyrus (20), and behavioral deficits consistent with abnormal functions of the amygdala, hippocampus, and cerebellum (19).

We recently reported that *Klf9* mRNA and protein were strongly induced in *Xenopus* brain by exposure to confinement/shaking stressor, which was blocked by treatment with mifepristone (RU486), or mimicked by injection of corticosterone (CORT) (23). Datson *et al.* (11) recently found *Klf9* to be induced by CORT in primary rat hippocampal neurons, and they provided evidence for two putative GR/MR binding sites in the *Klf9* 5′-flanking region. In the current study, we investigated the molecular basis for CORT regulation of *Klf9* in mouse hippocampal neurons. We looked at whether CORT could induce *Klf9* expression in mouse hippocampus *in vivo*, and in mouse hippocampal tissue culture cells, and we identified two evolutionarily conserved hormone-response elements in the *Klf9* 5′-flanking region to which the GR/MR bind to regulate *Klf9* expression.

Materials and Methods

Animal care

We purchased adult wild-type C57/BL6J mice from The Jackson Laboratory (Bar Harbor, ME), and Dr. Fujii-Kuriyama kindly provided *Klf9* mutant mice (*Klf9* locus disrupted by insertion of LacZ) (19). Mice were maintained on a 12-h light, 12-h dark photoperiod, given food and water *ad libitum*, and bred in the laboratory. We conducted histochemical staining for β-galactosidase using brains from 7-wk-old heterozygous *Klf9* mutant mice. Wild-type mice of mixed sex at PND 6 or 30 were given ip injections of CORT (Sigma Chemical Co., St. Louis, MO) dissolved in corn oil vehicle at 14 mg/kg body weight; this dose is in the midrange of CORT doses reported in the literature to increase plasma CORT (24). Control animals received vehicle or were unhandled. One hour after injection, animals were killed, and blood plasma and brains collected for analysis. We analyzed plasma [CORT] by radioimmunoassay as described (25, 26). We microdissected the hippocampal region for *Klf9* mRNA and heteronuclear RNA (hnRNA) analysis by RTqPCR (reverse transcription quantitative PCR). All experiments were conducted in accordance with the guidelines of the University Committee on the Use and Care of Animals at the University of Michigan.

RNA extraction, RT, and quantitative PCR

We extracted total RNA from HT-22 cells or the hippocampal region of PND 6 and 30 mice using the TRIzol reagent (Invitrogen Life Technologies, Carlsbad, CA) following the manufacturer's protocol. We treated 1 μg of total RNA with 20 U of ribonuclease-free deoxyribonuclease (DNAse) I (Roche, Indianapolis, IN) (27) before cDNA synthesis with the High Capacity Reverse Transcription kit (Invitrogen) with or without the addition of RT. For quantitative PCR, we designed TaqMan assays and conducted real-time PCR using ABsolute QPCR Low ROX Mix (ABgene Thermo Scientific, Surrey, UK). The *Klf9* mRNA TaqMan assay spanned an exon/intron boundary, whereas the *Klf9* hnRNA assay targeted the single intron (Supplemental Table 1, published on The Endocrine Society's Journals Online web site at http://endo.endojournals.org). Treatment of RNA with DNAse I removed genomic DNA contamination, which was confirmed by the inclusion of −RT controls in the hnRNA analysis. Standard curves were constructed with a cDNA pool from HT-22 cell RNA to compare relative expression levels. *Klf9* mRNA was normalized to *GAPDH* (TaqMan Assay no. 4352662; Applied Biosystems, Carlsbad, CA) mRNA, the expression of which did not change with hormone treatment.

Plasmid constructs

A chromatin immunoprecipitation (ChIP)-promoter DNA chip (ChIP-chip) assay for MR on chromatin from HEK293 cells that express myc-tagged human MR (HEK293-hMR+; for methods see Ref. 28) identified two regions of the upstream region of human *Klf9* (Ziera, T., and S. Borden, unpublished data). Bioinformatic analysis revealed that both loci contain putative GR/MR response elements (GRE/MRE). These regions were isolated from human genomic DNA by PCR (Supplemental Table 2); one was 632 bp from −5771 to −5139 bp (fragment 1, centered at ~5.5kb), a second was 336 bp from −4211 to −3875 bp (fragment 2, centered at ~4 kb) relative to the transcription start site (TSS). DNA fragments were subcloned into the pGL4.23 vector (Promega, Madison, WI) at the *Xho*I and *Hin*dIII sites for testing in HEK293-hMR+ cells (Supplemental Materials and Methods). The two orthologous regions of the mouse *Klf9* gene, a 634-bp fragment (fragment 1) located −5776 to −6410 bp relative to the TSS and a 336-bp fragment (fragment 2) located −4566 to −4892 bp relative to the TSS, were isolated from mouse genomic DNA by PCR and subcloned into pGL4.23. An evolutionarily conserved 179-bp mouse genomic region (−5333 to −5154 bp relative to the TSS) that contained a GRE/MRE identified by DNAse I footprinting (described below) was

also isolated by PCR and subcloned into pGL4.23. We also isolated and subcloned into pGL4.23 a 1269-bp fragment of the mouse *Klf9* gene (−6409 to −5140 relative to the TSS) spanning fragment 1 and the 179-bp evolutionarily conserved region. This construct included the two GRE/MRE at −6.1 and −5.3 kb described below. Plasmid constructs containing genomic DNA fragments with mutated GRE/MRE half-sites were generated using the QuikChange Site-Directed Mutagenesis kit (Agilent Technologies, Santa Clara, CA) following the manufacturer's protocol (Supplemental Table 3).

Cell culture and transient transfection assays

HT-22 is a cell line derived from mouse hippocampus immortalized with the simian virus 40 T antigen (29, 30) with properties of differentiated neurons (29–32). HT-22 expresses functional GR but has no detectable MR, because [^{3}H]-CORT binding in HT-22 lysates is completely displaced by RU486 (Rozeboom, A., and A. Seasholtz, unpublished data). HT-22/MR16 cells were engineered to express mouse MR by stably transfecting HT-22 cells with cytomegalovirus (CMV)-MR and pPGKpuro plasmids, and selection in 2.5 μg/ml puromycin. The CMV-MR construct contains the full-length mouse MR cDNA [clone pMR-2A (33) in pCMVneo]. The HT-22/MR16 cells exhibit MR binding and transcriptional activation of GRE-luciferase constructs with 1–10 nM aldosterone (ALDO) (Rozeboom, A., and A. Seasholtz, unpublished data).

We cultured HT-22 and HT-22/MR16 cells in DMEM (Invitrogen) supplemented with sodium bicarbonate (2.2 g/liter), penicillin G (100 U/ml), streptomycin sulfate (100 μg/ml), and 10% fetal bovine serum (FBS) stripped of thyroid (34) and steroid hormones (35). Cells were cultured under a humidified atmosphere of 5% CO_2 at 37 C. For gene expression analysis, we seeded cells at 2.5×10^6 per well in six-well plates; for transient transfection assays, we seeded cells at 6.5×10^4 per well in 24-well plates. At 80% confluency, and immediately before hormone treatments, we replaced the growth medium with serum-free DMEM. CORT (Sigma C2505), dexamethasone (DEX) (Sigma D1756), or ALDO (Sigma A9477) was dissolved in 100% ethanol and added to media to the final concentrations indicated below. RU486 (a GR antagonist; Sigma M8046) was dissolved in ethanol and added to wells to a final concentration of 0.5 or 1 μM 1 h before hormone addition. Spironolactone (SPR) (a MR antagonist; Sigma S3378) was dissolved in ethanol and added to wells to a final concentration of 0.5 μM 1 h before hormone addition. T_3 (Sigma T2752) was dissolved in dimethylsulfoxide. Control treatments received an equivalent concentration of vehicle (0.001% ethanol and 0.03% dimethylsulfoxide). All hormone treatments were continued for 4 h before cell harvest. Hormone treatment experiments were conducted at least two times with comparable results.

To determine whether hormone-dependent induction of *Klf9* mRNA requires ongoing protein synthesis, we treated cells with 100 μg/ml of cycloheximide (CHX) (Sigma Chemical Co.). This dose of CHX reduced protein synthesis by 98% in HT-22 cells (Bagamasbad, P., and R. Denver, unpublished data). We treated cells with CHX for 1 h before and during hormone treatment.

For luciferase reporter assays, we plated HT-22 cells in DMEM with hormone-stripped FBS and transfected at 50–60% confluency with 300 ng of the pGL4.23 reporter constructs plus 20 ng of p*Renilla* plasmid using the FuGENE 6 transfection reagent (Roche). Immediately before transfection, the growth medium was replaced with medium containing hormone-stripped FBS without penicillin/streptomycin, and cells were incubated with the transfection mixture overnight. Twenty-four hours after transfection, cells were changed to serum-free medium containing 100 nM CORT or vehicle for 4 h before harvest for luciferase activity using the dual luciferase assay kit (Promega). Each transfection experiment was conducted at least three times with four to five wells per treatment.

Electrophoretic mobility shift assay

We conducted EMSA as described (36) with recombinant human GR (hGR) generated using the TnT SP6 Quick Coupled Translation System (Promega). We programmed the reaction with 1 μg of CMV-hGR expression plasmid (OriGene, Rockville, MD) and confirmed protein expression (36). One microgram of duplex oligonucleotides (corresponding to the predicted GRE/MRE at −6.1 and −5.3 kb upstream of the TSS) (Supplemental Table 2) was labeled with ^{32}P-dCTP by Klenow fill-in for use as probes (50 K cpm/reaction) in EMSA. We conducted competitive EMSA with 1.5 μM radioinert (~1000-fold excess) wild-type or mutant GRE/MRE oligonucleotides (Supplemental Table 2). A ^{32}P-labeled mouse mammary tumor virus (MMTV) probe containing a well-characterized GRE was used as positive control for GR binding (Supplemental Table 3).

Fluorescent DNAse I footprinting

We conducted DNAse I footprinting as described (37) using the Promega Core Footprinting System protocol. We generated FAM or HEX fluorescent-labeled double-stranded DNA probes corresponding to the mouse *Klf9* 5′-flanking region (−5333 to −5154 bp; 179 bp). The region corresponding to the DNA binding domain (DBD) of the hGR was PCR amplified and subcloned into TOPO/pET151/D (Invitrogen) to make TOPO/pET151/D-hGR-DBD. Bacterially expressed GR-DBD was purified using ProBond (Invitrogen). We combined 1 μg of GR-DBD with 150 ng of HEX (green)-labeled probe in a 50-μl digestion reaction. The FAM (blue)-labeled probe (150 ng) was digested in a 50 μl of reaction without added GR-DBD. The two probe digestion reactions were then combined, extracted with phenol/chloroform, concentrated by ethanol precipitation, and analyzed by Big Dye Terminator Cycle sequencing (Applied Biosystems). Peaks in the chromatograms were assigned to specific nucleotides using FAM-labeled ddATP, ddCTP, ddGTP, or ddTTP in a manual sequencing reaction.

ChIP assay

We plated HT-22 cells in 100-mm plates in DMEM with hormone-stripped FBS. Cells at 90% confluency were treated with 100 nM CORT or ethanol vehicle in serum-free medium for 4 h before harvest for chromatin extraction. We also isolated chromatin from the hippocampal region of PND 6 mice 1 h after injection of CORT (14 mg/kg); control animals were left unhandled. Five micrograms of sheared chromatin were used for each reaction, and ChIP assay was conducted as described (16). Polyclonal rabbit antiserum to mouse GR (5 μg, M-20X; Santa Cruz Biotechnology, Inc., Santa Cruz, CA), histone 3 (H3) (07-690, 5 μl; Millipore, Billerica, MA), or antiacetylated H3 (AcH3) (06-599, 5 μl; Millipore) was used for ChIP assay. ChIP samples were analyzed by quantitative real-time PCR using TaqMan

primer/probe sets (Supplemental Table 1) targeted to different regions of the mouse *Klf9* gene.

Data analysis and statistics

We analyzed data by one-way ANOVA followed by Tukey's pairwise comparisons test, or by Student's *t* test using the SYSTAT computer program (version 10; SPSS, Inc., Chicago, IL). Data from dual luciferase assays (firefly luciferase counts divided by Renilla luciferase counts) and ChIP assays (the ratio of ChIP signal to input) were $\log_{10}$ transformed before statistical analysis. $P < 0.05$ was accepted as statistically significant. Gene expression data are reported as the mean ± SEM. To predict putative GRE/MRE sites, we used the online programs Transcription Element Search System (TESS) (www.cbil.upenn.edu) and Match (www.gene-regulation.com/pub/programs.html#match) using a library of matrices from TRANSFAC 6.0 (www.gene-regulation.com) with core and matrix similarity of transcription factor binding sites set higher than 0.85. The conservation of the identified GRE/MRE and flanking sequences was assessed using BLAT (http://genome.ucsc.edu/). Extracted sequences were aligned using ClustalW. The percent similarity to mouse was calculated for the GRE/MRE half-sites, and nucleotide frequency diagrams were produced with Weblogo (http://weblogo.berkeley.edu/logo.cgi).

Results

Exogenous CORT increased *Klf9* mRNA and hnRNA in mouse hippocampus *in vivo*

The *Klf9* gene is expressed in all regions of the mouse hippocampus (Fig. 1A) (19). Intraperitoneal injection of CORT in PND 6 or 30 mice increased *Klf9* mRNA [PND 6: $F_{(2,26)} = 17.084$, $P < 0.0001$; PND 30: $F_{(2,14)} = 6.937$, $P < 0.01$; ANOVA] (Fig. 1B) and hnRNA [PND 6: $F_{(2,26)} = 10.71$, $P < 0.001$; PND 30: $F_{(2,14)} = 27.427$, $P < 0.01$] (Fig. 1C) in the region of the hippocampus 1 h after injection compared with unhandled or vehicle-injected controls. CORT injection elevated plasma [CORT] above controls [$F_{(2,13)} = 7.353$, $P < 0.013$]; the vehicle-injected and unhandled groups were not significantly different from each other (unhandled, 48.9 ± 10.2 ng/ml; vehicle, 33.5 ± 9.9 ng/ml; and CORT, 1996 ± 830 ng/ml).

CORT caused a rapid and dose-dependent increase in *Klf9* mRNA in HT-22 cells

CORT increased *Klf9* mRNA in HT-22 cells in a time- and dose-dependent manner [time: $F_{(5,23)} = 22.06$, $P < 0.0001$; dose: $F_{(7,30)} = 37.69$, $P < 0.0001$; ANOVA] (Fig. 2, A and B); *Klf9* hnRNA was also increased by CORT ($P < 0.05$; Student's *t* test) (Fig 2C). The mean *Klf9* mRNA level was higher at 30 min after CORT exposure, was statistically significant at 1 h and was maximal by 2 h. The EC_{50} (measured at 4 h) was 5.7 nM, and maximal response was at 30 nM. *Klf9* is a direct thyroid hormone receptor target gene in rodent and frog (15, 16, 36, 38). For comparison with the CORT response, we show that *Klf9* is

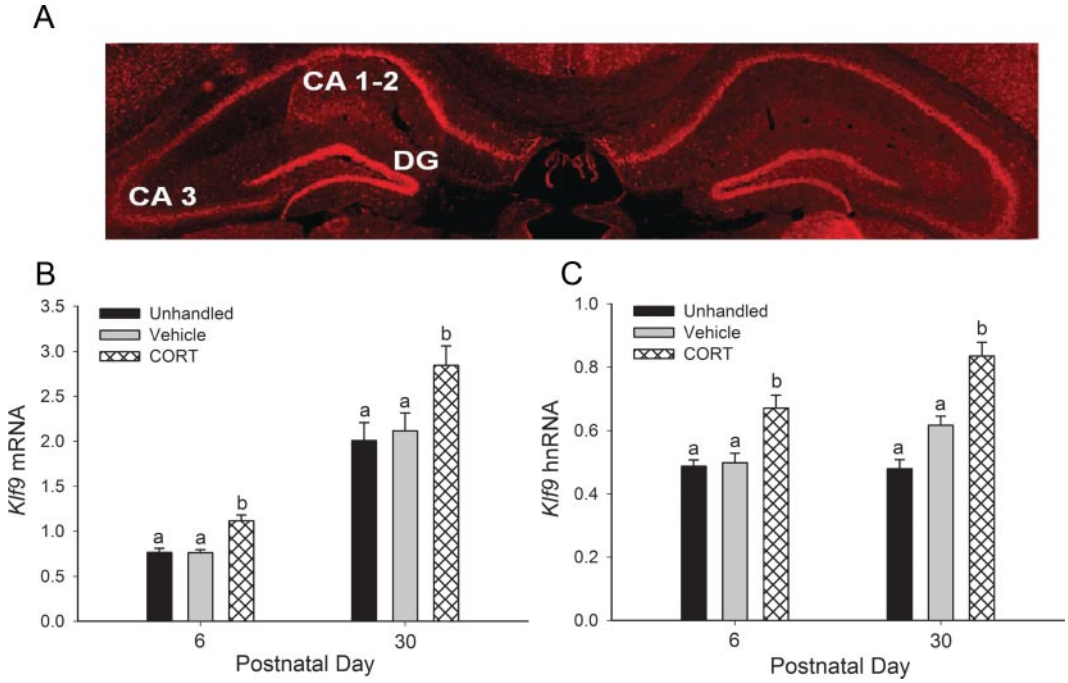

FIG. 1. Injection of CORT increased *Klf9* mRNA and hnRNA levels in the hippocampal region of the postnatal mouse brain. A, A representative coronal section of the hippocampal region of a LacZ-*Klf9* heterozygous mouse generated by insertion of LacZ within the coding region of the *Klf9* gene (19). Histochemistry was conducted for β-galactosidase with immunofluorescent detection using Cy3. B, PND 6 and 30 wild-type C57/BL6J mice were injected with vehicle (oil), CORT at a dose of 14 mg/kg bodyweight, or left unhandled. One hour after injection, animals were killed, the hippocampal region was dissected, and RNA extracted for measurement of *Klf9* mRNA by RTqPCR (n = 8 at PND 6 and n = 5 at PND 30). C, PND 6 mice were injected with CORT as described above, and *Klf9* hnRNA was measured by RTqPCR (n = 8). *Klf9* mRNA and hnRNA were normalized to the mRNA level of the housekeeping gene *GAPDH*. *Bars* represent the mean ± SEM, and *letters above the means* indicate significant differences among treatments (means with the *same letter* are not significantly different; Tukey's pairwise comparisons test; $P < 0.05$). DG, Dentate gyrus.

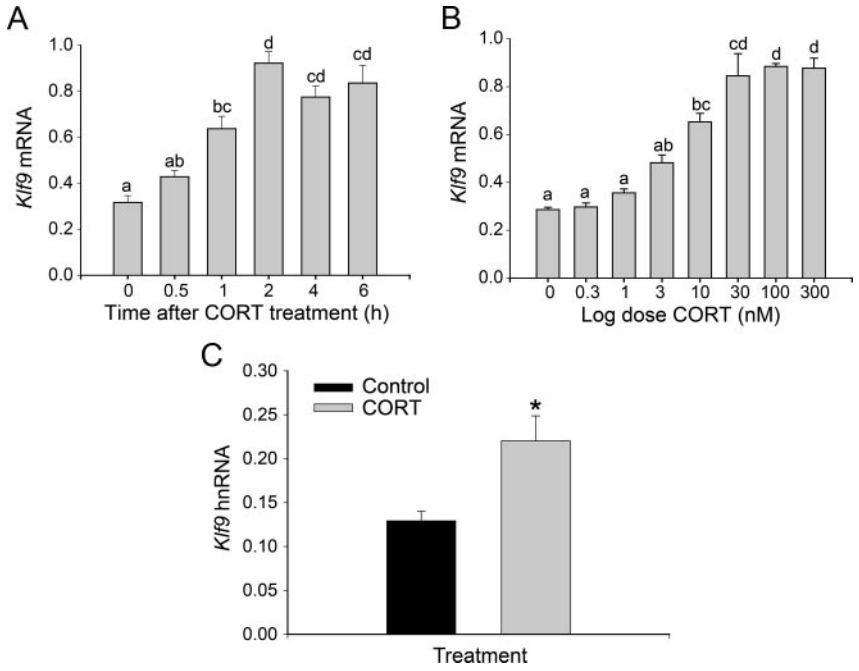

FIG. 2. Treatment with CORT caused dose- and time-dependent increases in *Klf9* mRNA in the mouse hippocampal-derived cell line HT-22. HT-22 cells were treated with 100 nM CORT for different times (A) or with increasing doses of CORT for 4 h (B) before harvest and analysis of *Klf9* mRNA. C, HT-22 cells were treated with 100 nM CORT for 4 h before harvest and analysis of *Klf9* hnRNA. In each experiment, HT-22 cells were treated with the hormone doses for the times indicated before cell harvest, RNA extraction, and analysis by RTqPCR. *Klf9* mRNA and hnRNA were normalized to the mRNA level of the housekeeping gene *GAPDH*. *Bars* represent the mean ± SEM (n = 4), and *letters above the means* indicate significant differences among hormone concentrations or time point (means with the *same letter* are not significantly different; Tukey's pairwise comparison test; $P < 0.05$). *, $P < 0.05$ (Student's *t* test).

regulated by T_3 in a time- and dose-dependent manner in HT-22 cells (Supplemental Fig. 1).

Hormone induction of *Klf9* mRNA in HT-22 cells was resistant to protein synthesis inhibition, supporting that *Klf9* is a direct hormone-response gene [control (−CHX): $F_{(2,11)} = 81.63$, $P < 0.0001$; CHX: $F_{(2,11)} = 151.8$; $P < 0.001$; ANOVA] (Fig. 3A).

Both GR and MR can regulate the *Klf9* gene, but the GR may predominate

CORT (100 nM) or the GR-selective agonist DEX (10 nM) caused similar increases in *Klf9* mRNA (~3-fold) measured at 4 h [−RU486: $F_{(2,11)} = 42.40$, $P < 0.001$; ANOVA] (Fig. 3B) that could be blocked by cotreatment with the GR receptor antagonist RU486 [+RU486, $F_{(2,11)} = 3.128$] (Fig. 3B). These data support that *Klf9* can be regulated by the GR in HT-22 cells, but they do not exclude a role for MR in *Klf9* regulation in other cell types, because HT-22 cells do not express functional MR (Rozeboom, A. M., and A. F. Seasholtz, unpublished data). Consistent with a lack of functional MR, HT-22 cells did not respond to ALDO (10 nM) (Fig. 3C).

To determine whether the MR can mediate corticosteroid actions on *Klf9* gene expression, we analyzed hormone responses in HT-22/MR16 cells. A dose of 1 nM ALDO activated a GRE/MRE-containing promoter-reporter construct in these cells [Rozeboom, A., and A. F. Seasholtz, unpublished data; the Kd for ALDO binding to MR is 0.5–2.6 nM (3, 39, 40)]. ALDO (10 nM) caused a small, but statistically significant, increase in *Klf9* mRNA [$F_{(8, 27)} = 26.45$, $P < 0.001$; ANOVA] (Fig. 3C). The response to ALDO was dose dependent with an EC_{50} of 25 nM [$F_{(8,35)} = 26.45$, $P < 0.001$] (Fig. 3D). This EC_{50} is approximately five times greater than the EC_{50} for CORT in HT-22 cells; ALDO concentrations more than 30 nM can activate the GR (41).

To further investigate the contributions of GR *vs.* MR in the regulation of *Klf9*, we treated HT-22/MR16 cells with 25 nM CORT or ALDO with or without the GR-specific antagonist RU486 (500 nM), the MR-specific antagonist SPR (500 nM), or RU486 plus SPR (Supplemental Fig. 2). We chose a dose of 25 nM for both hormones, because this dose is the EC_{50} for ALDO action on *Klf9* mRNA in HT-22/MR16 cells. Treatment with RU496 plus SPR in the absence of hormone caused a small, but statistically significant, elevation in *Klf9* mRNA [$F_{(3,11)} = 8.784$, $P < 0.01$]. Both CORT and ALDO increased *Klf9* mRNA [$F_{(2,11)} = 27.891$, $P < 0.0001$; ANOVA], although the response to ALDO was significantly lower than for CORT ($P < 0.001$; Tukey's). RU486 reduced the response to CORT ($P < 0.01$; Tukey's) but did not affect the ALDO response, supporting that the action of ALDO is via the MR. The mean CORT and ALDO responses were lower in the presence of SPR but were not statistically significant. RU486 plus SPR reduced the response to CORT [$F_{(3,15)} = 8.073$, $P < 0.01$], which was significantly lower than SPR alone but was not significantly different from RU486 alone, supporting that the major action of CORT on *Klf9* is via the GR. The effect of cotreatment with RU486 plus SPR on the ALDO response was not different from SPR alone.

Identification of functional GRE/MRE in the human and mouse *Klf9* genes

A ChIP-chip assay for MR on chromatin from HEK293-hMR+ cells identified two MR binding sites in the 5′-flank-

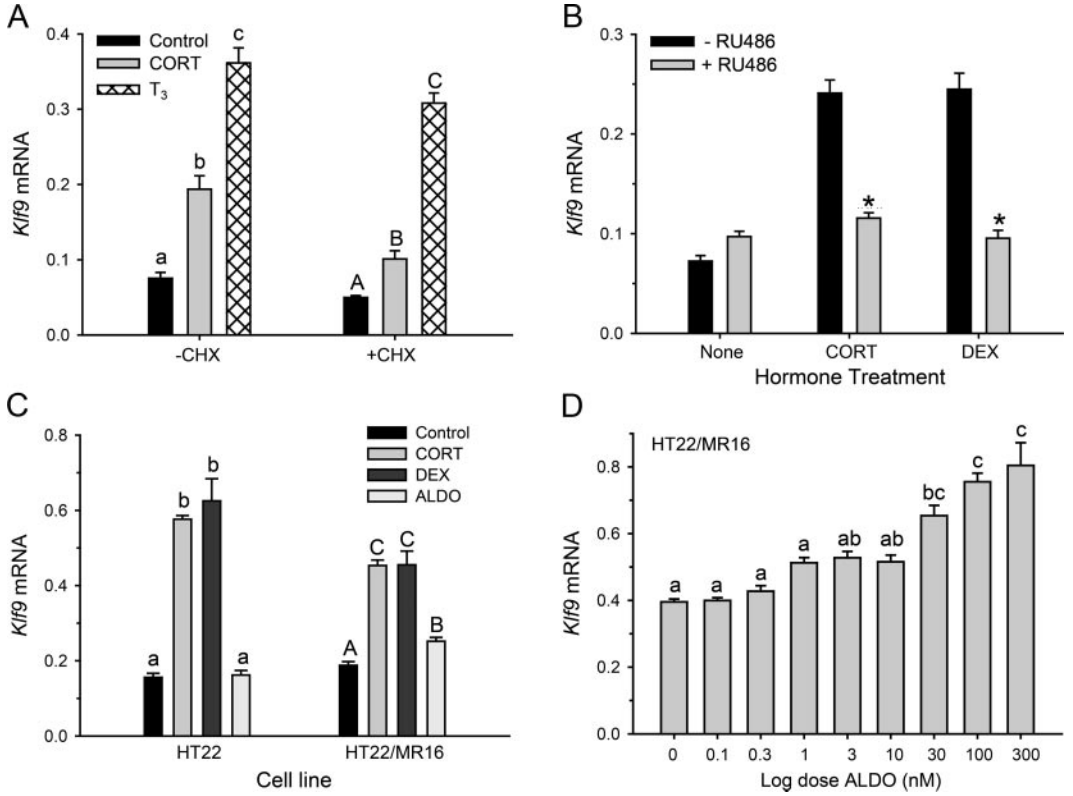

FIG. 3. Induction of *Klf9* mRNA by CORT in HT-22 cells is resistant to protein synthesis inhibition. *Klf9* can be regulated by the GR or by the MR. A, HT-22 cells were treated with or without CHX (100 μg/ml) for 30 min before addition of CORT (100 nM) or T_3 (30 nM). Treatment with CHX plus hormones was continued for 4 h before cell harvest for analysis of *Klf9* mRNA. We used T_3 as a positive control, because earlier we showed that *Klf9* is a direct TR target gene (16). B, HT-22 cells were cultured in the presence or absence of the GR-selective antagonist RU486 (1 μM) for 1 h before the addition of vehicle (100% EtOH), 100 nM CORT, or 10 nM of the GR-selective agonist DEX. Hormone treatment was continued for 4 h before cell harvest and analysis of *Klf9* mRNA. C, HT-22 and HT-22/MR16 cells were treated with vehicle (100% EtOH), 100 nM CORT, 10 nM DEX, or 10 nM ALDO for 4 h before cell harvest for analysis of *Klf9* mRNA. D, HT-22/MR16 were treated with increasing concentrations of the MR-selective agonist ALDO for 4 h before cell harvest for analysis of *Klf9* mRNA. In each experiment, cells were treated with the hormone doses for the times indicated before cell harvest, RNA extraction, and gene expression analysis by RTqPCR. *Klf9* mRNA was normalized to the mRNA level of the housekeeping gene *GAPDH*. *Bars* represent the mean ± SEM (n = 4), and *letters above the means* indicate significant differences among hormone concentrations or time point (means with the *same letter* are not significantly different; Tukey's pairwise comparison test; $P < 0.05$). *, $P < 0.05$ (Student's *t* test).

ing region of the human *Klf9* gene (Ziera, T., and S. Borden, unpublished data). One region (fragment 1) was centered at approximately −5.5 kb and a second (fragment 2) at approximately −4 kb relative to the TSS. Both regions were cloned into pGL4.23 to determine whether these regions support corticosteroid-dependent transcriptional activation. Enhancer-reporter assays in HEK293-hMR+ cells showed that only fragment 1 was activated by ALDO, and this response was blocked by the MR-specific antagonist RU26752 (Supplemental Fig. 3). This genomic region is highly conserved between human and mouse. *In silico* analysis of the human *Klf9* fragment 1 using TESS and Match identified a near perfect palindromic GRE/MRE full site that is completely conserved between mouse (*mKlf9* GRE/MRE 6.1) and human (−5474 bp in human, *hKlf9* GRE/MRE 5.5; Fig. 4A, partial sequence of the 600-bp fragment shown). The GR bound the mouse *Klf9* GRE/MRE-6.1 probe in EMSA, and this binding was competed by radioinert wild-type, but not mutant, GRE/MRE-6.1 oligonucleotide, thus confirming the specificity of binding (Fig. 4B).

We cloned the region of the mouse *Klf9* gene (*mKlf9* 634-bp fragment, −6410 to −5776 bp) orthologous to human fragment 1 and compared the ability of the mouse and human sequences to support CORT-dependent transactivation in transient transfection assays in HT-22 cells. Both the human and mouse *Klf9* gene fragments supported CORT-dependent transactivation (*hKlf9* GRE/MRE-5.5, 3.3-fold activation, $P < 0.0001$; *mKlf9* GRE/MRE-6.1, 2.6-fold activation, $P < 0.0001$; Student's *t* test) (Fig. 4C). Mutation of each half-site of the mouse *Klf9* GRE/MRE-6.1 abolished CORT responsiveness (Fig. 4C).

Earlier we found stressor and CORT-dependent regulation of the *Klf9* gene in *Xenopus* (23), but we were unable to identify a GRE/MRE in a similar region of the frog gene (*Xenopus tropicalis* genome version 4.1). In a sepa-

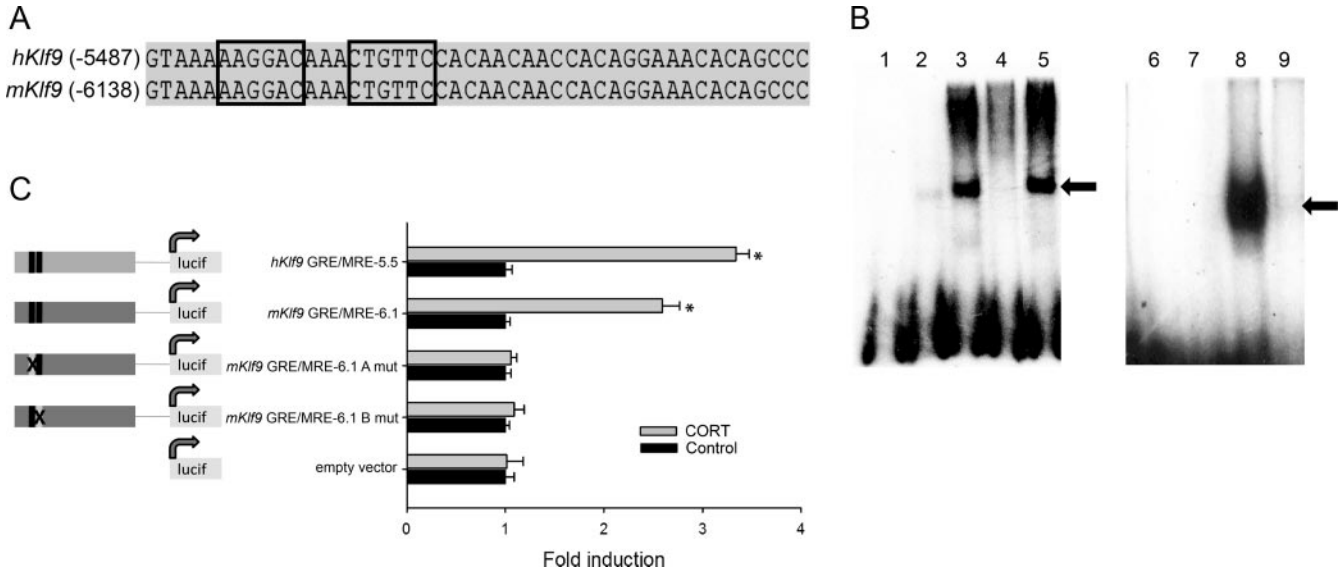

FIG. 4. Identification and functional analysis of a GRE/MRE located at −5.5 kb in the human and −6.1 kb in the mouse *Klf9* genes. A, A ChIP-chip promoter assay conducted on chromatin isolated from HEK293-hMR+ cells identified a fragment of approximately 600 bp in the human *Klf9* 5′-flanking region that contains a functional GRE/MRE (Ziera, T., and S. Borden, unpublished data). The sequence alignment is of a portion of this genomic region of human and mouse *Klf9* showing the presence of putative GRE/MRE sites in the two genes (half-sites are *boxed*) predicted by the TESS and Match programs. The numbers to the *left* of the alignment indicate the positions upstream of the TSS. The GRE/MRE in the human gene is centered at approximately −5.5 kb, and the GRE/MRE in the mouse gene is centered at approximately −6.1 kb. B, The ability of the GR to bind to the mouse *Klf9* GRE/MRE-6.1 *in vitro* was tested by EMSA. Each reaction contained [^{32}P]-labeled GRE/MRE-6.1 oligonucleotide as probe (lanes 1–5) and 2 μl of *in vitro*-synthesized luciferase protein (control, lane 2) or hGR protein (lanes 3–5). The GR binding to the probe was competed with 1.5 μM radioinert GRE/MRE-6.1 (lane 4) or mutant GRE/MRE-6.1 oligonucleotides (lane 5). We conducted EMSA with a MMTV GRE probe as a positive control for GR binding (*right panel*). Each reaction contained [^{32}P]-labeled MMTV oligonucleotide as probe (lanes 6–9) and 2 μl of *in vitro*-synthesized luciferase protein (negative control, lane 7) or hGR protein (lanes 8 and 9). The GR binding to the MMTV probe was competed with 1.5 μM radioinert MMTV oligonucleotide (lane 9). The supershifted bands indicated by the *arrows* are the GR-bound probe. C, pGL4.23 reporter constructs containing the human GRE/MRE-5.5, mouse GRE/MRE-6.1, and corresponding half-site mutants (X; A, 5′half-site and B, 3′half-site) of the mouse GRE/MRE-6.1 were transfected into HT-22 cells. Cells were treated with CORT for 4 h before harvest and analysis by dual luciferase assay. *Bars* represent the mean ± SEM (n = 5). *Asterisks* indicate statistically significant differences between vehicle (control) and CORT-treated cells for each enhancer-reporter construct ($P < 0.0001$; Student's *t* test).

rate study looking for CORT-responsive regions of the frog *Klf9* gene, we discovered that a region −6 to −5 kb relative to the TSS was CORT responsive (Bagamasbad, P., and R. J. Denver, unpublished data). Sequence comparison revealed an approximately 180-bp sequence within this region that was highly conserved between frog and mammalian *Klf9* genes. This region of the frog *Klf9* gene was previously reported to possess a T_3-response element (T_3RE) (42). Through DNAse I footprinting with GR-DBD of the orthologous mouse genomic region (179-bp fragment), we identified a GRE/MRE full site that is highly conserved across tetrapods (centered at −5285 bp in mouse, −4634 bp in human, and −5957 bp in frog *Klf9* genes) (Fig. 5, A and B). We designated this mouse GRE/MRE-5.3 and confirmed that GR bound this sequence in EMSA (Fig. 5C). Binding of GR to the GRE/MRE-5.3 probe was competed by radioinert wild-type, but not by mutant, GRE/MRE-5.3 oligonucleotide, thus confirming the specificity of binding (Fig. 5C). The 179-bp fragment of the mouse *Klf9* gene supported CORT-dependent transactivation in enhancer-reporter assays in HT-22 cells (Fig. 5D). Mutation of both half-sites of the GRE/MRE-5.3 reduced, but did not eliminate, CORT-dependent transactivation ($P < 0.05$, Student's *t* test) (Fig. 5D). The CORT-dependent activity of an enhancer-reporter plasmid containing a 1269-bp *Klf9* DNA fragment spanning the two identified GRE/MRE sites was not different from plasmids containing the individual response elements (Supplemental Fig. 4).

ChIP assay conducted with chromatin extracted from the hippocampal region of PND 6 mice showed GR association at both the GRE/MRE-6.1 and GRE/MRE-5.3 regions, which was increased by CORT injection ($P < 0.05$, Student's *t* test) (Fig. 6A). By comparison, there was no significant GR ChIP signal at the *Klf9* intronic region (+11 kb from the TSS). In HT-22 cells, AcH3 was substantially greater at the two GRE/MRE regions compared with the intron. Treatment of cells with CORT for 4 h increased H3 acetylation at the GRE/MRE-5.3 ($P < 0.01$, Student's *t* test) but not at the GRE/MRE- 6.1 or at the intron (Fig. 6B, *top panel*). Treatment with CORT decreased H3 association but only at the GRE/MRE-5.3 ($P < 0.01$, Student's *t* test) (Fig. 6B, *bottom panel*).

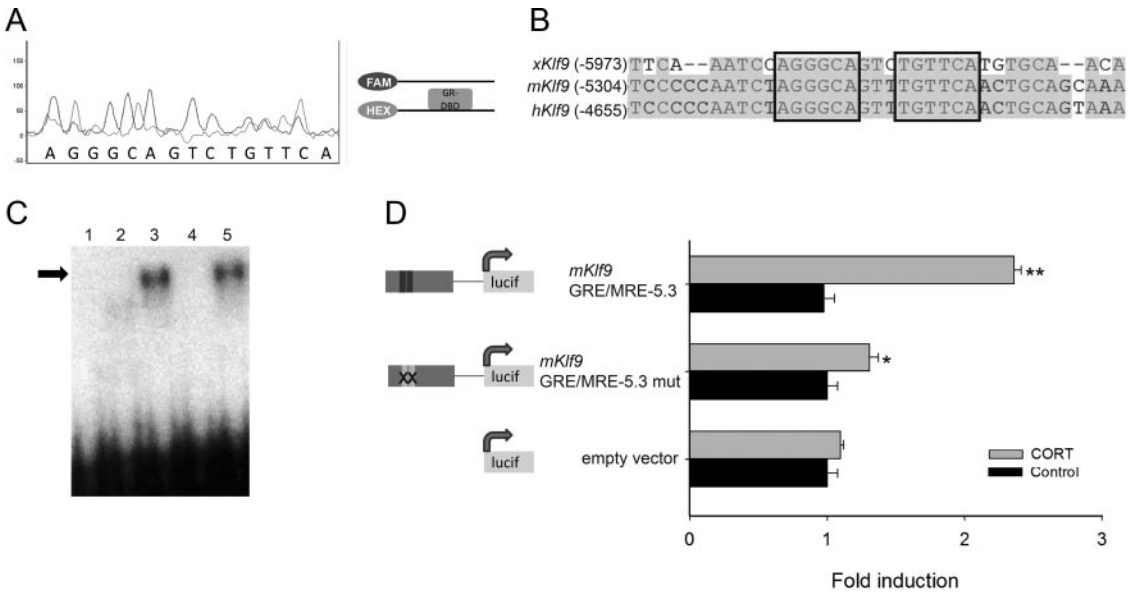

FIG. 5. Identification and functional analysis of an evolutionarily conserved GRE/MRE located at −5.3 kb in the mouse (−4.6 kb in the human) *Klf9* gene. A, DNAse I protection assay with the hGR-DBD of the evolutionary conserved 179-bp fragment of the mouse *Klf9* gene identified a GRE/MRE located approximately −5.3 kb relative to the TSS (see *Materials and Methods*). The *light gray traces* are from the probe incubated with the GR-DBD, whereas the *dark gray traces* are from the probe incubated without the GR-DBD. Areas where there is a *dark gray peak* but no *light gray peak* indicate nucleotides protected from DNAse I digestion by the GR-DBD. The nucleotide sequence is shown *beneath the traces*. B, Sequence alignment showing conservation of the GRE/MRE (mouse GRE/MRE-5.3) in human, mouse, and frog *Klf9* genes (GRE/MRE half-sites are *boxed*). The *numbers to the left* of the alignment indicate the positions upstream of the TSS. The GRE/MRE in the human gene is centered at approximately −4.6 kb and in the frog gene at approximately −5.9 kb. C, The ability of the GR to bind to the mouse *Klf9* GRE/MRE-5.3 was tested *in vitro* by EMSA. Each reaction contained [^{32}P]-labeled GRE/MRE-5.3 oligo as probe (lanes 1–5) and 2 μl of *in vitro*-synthesized luciferase protein (negative control, lane 2) or hGR protein (lanes 3–5). The GR binding to the probe was competed with 1.5 μM radioinert GRE/MRE-5.3 (lane 4) or mutant GRE/MRE-5.3 oligonucleotides (lane 5). The supershifted bands indicated by the *arrow* are the GR-bound probe. D, pGL4.23 reporter constructs containing the mouse GRE/MRE-5.3 and corresponding GRE/MRE-5.3 mutant (X) were transfected into HT-22 cells. Cells were treated with CORT for 4 h before harvest and analysis by dual luciferase assay. *Bars* represent the mean ± SEM (n = 5). *Asterisks* indicate statistically significant differences between vehicle (control) and CORT-treated cells for each enhancer-reporter construct (*, $P < 0.05$; **, $P < 0.0001$; Student's *t* test).

Evolutionary conservation of the GRE/MRE in vertebrate *Klf9* genes

Bioinformatic analysis of the two GRE/MRE identified in this study (−5.3 and −6.1 kb in mouse) showed that these sequences are highly conserved across species. Both half-sites of the mouse GRE/MRE-5.3 are identical across several orders of mammals, a representative lizard, and a frog (Fig. 7). There are two nucleotide substitutions in one of the half-sites in zebra finch. We located an orthologous region in galliform genomes (chicken and turkey), but the putative GRE/MRE sequences were highly divergent and included an insertion mutation in the half-site spacer region. We were unable to identify a region orthologous to GRE/MRE-5.3 in ray-finned fish. The GRE/MRE-6.1 is highly conserved across therian mammals, with only a single base substitution in a half-site between marsupials and eutherians (Fig. 7). This GRE/MRE occurs within an approximately 150-base region that is also mostly conserved across therians. We could not identify an orthologous region, nor a GRE/MRE-6.1 in the genomes of a monotreme (platypus), birds (zebra finch, chicken, and turkey), a lizard (anole), clawed frogs, or fish (puffer fish, zebra fish, or stickle back).

Discussion

Glucocorticoids exert profound and complex actions on the central nervous system, many of which are mediated by the GR and MR. However, the genes regulated by GR and MR, and roles for the protein products of these genes in central nervous system development and function, are poorly understood. Here, we describe the identification and functional characterization of two GRE/MRE in *Klf9*, a GC-inducible gene in hippocampal neurons that codes for a transcription factor known to play a role in neuronal structure and function (15, 19, 20, 22, 23, 43). We found that the mouse *Klf9* gene is induced by GC *in vivo* and in the hippocampal-derived cell line HT-22. The GR is recruited to *Klf9* upstream regions in a hormone-dependent manner, leading to histone acetylation and nucleosome eviction at the GRE/MRE-5.3, consistent with GC promoting an open chromatin structure at the *Klf9* locus. These results agree with our previous findings in *Xenopus*, where exposure to handling/shaking stressor or injection of CORT caused rapid increases in *Klf9* mRNA and protein in frog brain (23).

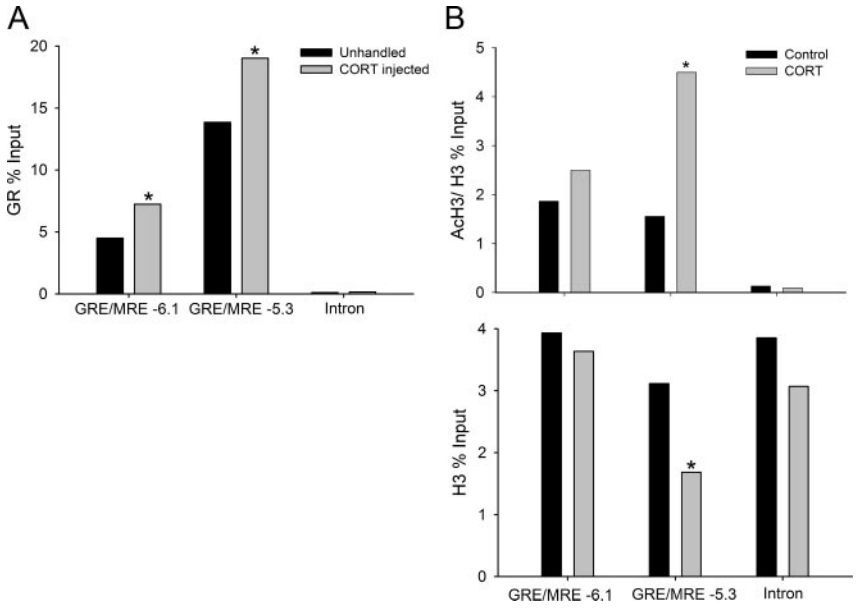

FIG. 6. CORT promotes GR association, H3 acetylation, and nucleosome eviction at the 5′-flanking region of the mouse *Klf9* gene. A, wild-type PND 6 mice were injected with CORT at a dose of 14 mg/kg bodyweight or left unhandled. One hour after injection, animals were killed, the hippocampal region was dissected, and chromatin extracted for GR ChIP assay. ChIP samples (n = 9) were analyzed by RTqPCR using TaqMan assays that targeted the GRE/MRE-6.1, GRE/MRE-5.3, or a distal intronic region (negative control) of the mouse *Klf9* gene. *Bars* represent the mean ChIP signals expressed as a percentage of input. Statistical analysis was conducted on $\log_{10}$-transformed data, and the *asterisks* indicate statistically significant differences between unhandled and CORT-injected animals ($P < 0.05$; Student's *t* test). B, HT-22 cells were treated with EtOH vehicle or 100 nM CORT for 4 h before harvest for chromatin extraction and ChIP assay for AcH3 (*top panel*) and H3 (*bottom panel*). ChIP samples (n = 4) were analyzed by RTqPCR using TaqMan assays that target the GRE/MRE-6.1, GRE/MRE-5.3, or a distal intronic region (negative control) of the mouse *Klf9* gene. *Bars* represent the mean ChIP signals expressed as a percentage of input. Statistical analysis was conducted on $\log_{10}$-transformed data, and the *asterisks* indicate statistically significant differences between vehicle (control) and CORT-treated cells ($P < 0.01$; Student's *t* test).

Increased levels of *Klf9* hnRNA in mouse brain *in vivo* and in HT-22 cells show that CORT increased transcription of the *Klf9* gene. Also, the rapid kinetics of CORT-dependent up-regulation of *Klf9* mRNA in HT-22 cells, and the resistance to protein synthesis inhibition, support that CORT regulation of *Klf9* transcription is direct. Regulation of *Klf9* by GR is supported by induction of *Klf9* mRNA by the GR-specific agonist DEX and blockade of DEX and CORT responses by the GR-specific antagonist RU486. These results parallel our findings in *Xenopus*, where stressor-induced increases in *Klf9* mRNA *in vivo*, or CORT-dependent responses in XTC-2 cells, were completely blocked by RU486 (23).

Our findings in mouse and frog support that *Klf9* is regulated by the GR. We also provide evidence that mammalian *Klf9* genes can be regulated by the MR, although the GR may predominate. ALDO caused a small, but significant, increase in *Klf9* mRNA in HT-22/MR16 cells. However, this induction was significantly less than the CORT-mediated increase. In addition, CORT-dependent induction of *Klf9* mRNA in HT-22/MR16 cells was blocked by the GR antagonist RU486 but not by the MR antagonist SPR. Taken together, we conclude that although the MR may contribute to the regulation of *Klf9*, this action is less important than the GR and may be dependent on the sequence of the GRE/MRE, the cell type, and perhaps the MR:GR ratio.

KLF9 is directly regulated by GC in hippocampal neurons via two GRE/MRE located in the 5′-flanking region of the gene. A ChIP-chip assay identified a GRE/MRE located at −5.5 kb in human *Klf9*, and we confirmed its presence in an orthologous region of the mouse genome (at −6.1 kb) and the functionality of this response element in both species. This sequence, comprising a GRE/MRE of two half-sites with a three base spacer (see Fig. 3B), was earlier found by So *et al.* (44) to be bound by GR in mouse $C^3H10T1/2$ mesenchymal stem-like cells. Comparative sequence analysis showed that the GRE/MRE-6.1 is conserved among several orders of therian mammals but is not found in monotremes or other vertebrates. Datson *et al.* (11) recently found that GR binds to this region in rat hippocampal cells. We extend their findings by showing that this sequence supports hormone-dependent transactivation, which is abolished by point mutation of the half-sites; that GR binds to this sequence *in vitro*; and that GR associates with this genomic region in a hormone-dependent manner *in vivo*. We also show the therian origin of this response element and conservation over more than 160 million years in mammals (Fig. 7).

We identified a second GRE/MRE located at −5.3 kb in the mouse *Klf9* gene (~800 bp downstream of the GRE/MRE-6.1). This region was not bound by MR in a ChIP-chip assay of chromatin isolated from HEK293-hMR+ cells (Ziera, T., and S. Borden, unpublished data); we identified it in a promoter-reporter scan of the *Xenopus Klf9* 5′-flanking region. The orthologous region of the mouse gene supported GC-dependent transactivation, so we conducted DNAse I footprinting and subsequently identified a GRE/MRE full site. The GRE/MRE-5.3 half-sites are 100% conserved across several mammalian orders, a lizard, and a frog. Datson *et al.* (11) recently found evidence for a GRE/MRE in this region of the rat *Klf9* gene. We extend their findings by confirming its functionality and

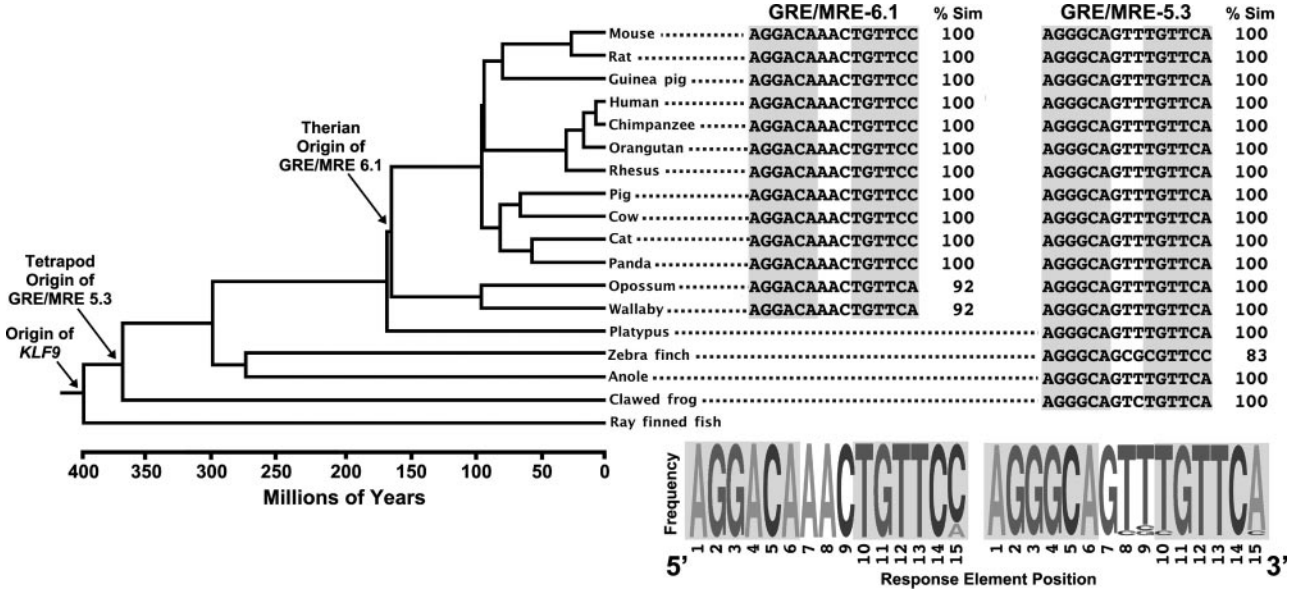

FIG. 7. Origin and evolution of two GRE/MRE in vertebrate *Klf9* genes. Phylogeny of vertebrate relationships with branch lengths scaled to average divergence time estimates (www.timetree.org). *Arrows* indicate the minimum origin of the *Klf9* gene, and *Klf9* GRE/MRE-5.3, and 6.1 (numbering based on the distance from the mouse *Klf9* TSS). The GRE/MRE sequences for each taxon are shown to the *right* of the tree (when present). Half-sites are highlighted, and their percent similarities (Sim) to mouse are listed. The frequency of each nucleotide position for the taxa shown is depicted *below* its respective GRE/MRE alignment.

high degree of conservation over 370 million years of tetrapod evolution.

The GRE/MRE-5.3 is found within an evolutionarily conserved genomic region of approximately 180 bp located −5 to −6 kb relative to the TSS in vertebrate *Klf9* genes. Outside of the coding region and the core promoter, there is no evolutionary conservation between frog and mammal *Klf9* genes, suggesting that this approximately 180-bp sequence has been subject to strong stabilizing selection. In *Xenopus*, this approximately 180-bp region was earlier found to contain a functional T_3RE, to which TR binds to induce *Klf9* expression during tadpole metamorphosis (42). We confirmed that the mouse has a homologous T_3RE [Bagamasbad, P., and R. J. Denver, unpublished data; in addition to a T_3RE at −3.8 kb relative to the TSS (16)]. The approximately 180-bp sequence also contains an evolutionarily conserved, predicted GRE/MRE half-site adjacent to the T_3RE. However, this region was not protected by GR-DBD in DNAse I footprint assay. It is possible that the GR associates with the region of the T_3RE through low-affinity DNA binding, or though protein-protein interactions, which could account for the residual CORT response observed when the GRE/MRE-5.3 was mutated.

ChIP assay showed greater GR association at the mouse GRE/MRE-5.3 compared with the GRE/MRE-6.1. This was accompanied by hormone-induced H3 acetylation at the GRE/MRE-5.3 but not at the GRE/MRE-6.1. H3 acetylation is a marker for transcriptionally active chromatin (8) and is necessary to promote nucleosome eviction and chromatin disassembly (45). Consistent with this, we observed hormone-dependent nucleosome eviction (depletion of H3) at the region of the GRE/MRE-5.3 but not at the GRE/MRE-6.1. Although the GR associates with the GRE/MRE-6.1 *in vivo* and *in vitro*, and this sequence can support hormone-dependent transactivation, our findings of GR recruitment and histone modification suggest that the GRE/MRE-5.3 may be a more significant hormone-response element *in vivo*. This may reflect the location of the GRE/MRE-5.3 within the conserved approximately 180-bp genomic region, where other proteins, such as the liganded TR, bind to *cis* regulatory elements to promote an open chromatin structure, thereby allowing for greater GR recruitment and action (Bagamasbad, P., and R. J. Denver, unpublished data).

GC actions on the hippocampus require new protein synthesis achieved though transactivation of GC target genes by liganded GR or MR. Recently, some GR/MR genomic targets have been identified in hippocampal neurons (*e.g.* Ref. 11), but little is known about the function of their gene products in hippocampal cell physiology and structure. Earlier we showed that KLF9 is in the pathway induced by TH that promotes differentiation of neuronal cells (15, 22, 23). Morita *et al.* (19) found that *Klf9* null mice had reduced dendritic arborization of cerebellar Purkinje cells and behavioral abnormalities consistent with defects of the hippocampus, cerebellum, and amygdala. These mice also displayed impaired late-phase adult hippocampal neurogenesis (20), a critical component of hippocampal-dependent learning and memory (46). Given

that structural plasticity of the hippocampus is regarded to be the basis for learning and memory (47) and that *Klf9* is regulated by corticosteroids and TH, and is highly expressed in the hippocampus, a brain region targeted by corticosteroids and influences neuronal morphology, we hypothesize that KLF9 functions as an important intermediate in the actions of stress and TH on hippocampal plasticity and consequently on learning and memory.

Acknowledgments

We thank Dr. Yoshiaki Fujii-Kuriyama (Japan Science and Technology Agency, Saitama, Japan) for providing the *Klf9*-LacZ mice and to Dr. David Schubert (Salk Institute, La Jolla, CA) for providing the HT-22 cells.

Address all correspondence and requests for reprints to: Robert J. Denver, Ph.D., 3065C Natural Science Building, Department of Molecular, Cellular, and Developmental Biology, The University of Michigan, Ann Arbor, Michigan 48109-1048. E-mail: rdenver@umich.edu.

This work was supported by the National Institute of Neurological Disorders and Stroke, National Institutes of Health Grant 1 R01 NS046690 and the National Science Foundation Grant IOS 0922583 (to R.J.D.). This research used the Cell and Molecular Biology Core of the Michigan Diabetes Research and Training Center funded by the National Institute of Diabetes and Digestive Kidney Diseases Grant NIHP60 DK20572. P.B. was supported by a predoctoral fellowship from the Rackham Graduate School and an Edwin Edwards Scholarship from the Department of Molecular, Cellular, and Developmental Biology, University of Michigan. A.M.R. was supported in part by the National Institutes of Health Cellular and Molecular Biology Training Grant T32-GM007315 at the University of Michigan.

Disclosure Summary: The authors have nothing to disclose.

References

1. **Joëls M, Pu Z, Wiegert O, Oitzl MS, Krugers HJ** 2006 Learning under stress: how does it work? Trends Cogn Sci 10:152–158
2. **McEwen BS** 2008 Central effects of stress hormones in health and disease: understanding the protective and damaging effects of stress and stress mediators. Eur J Pharmacol 583:174–185
3. **Reul JM, de Kloet ER** 1985 Two receptor systems for corticosterone in rat brain: microdistribution and differential occupation. Endocrinology 117:2505–2511
4. **De Kloet ER, Vreugdenhil E, Oitzl MS, Joëls M** 1998 Brain corticosteroid receptor balance in health and disease. Endocr Rev 19: 269–301
5. **Puymirat J** 1992 Thyroid receptors in the rat brain. Prog Neurobiol 39:281–294
6. **Aranda A, Pascual A** 2001 Nuclear hormone receptors and gene expression. Physiol Rev 81:1269–1304
7. **Ribeiro RC, Kushner PJ, Baxter JD** 1995 The nuclear hormone receptor gene superfamily. Annu Rev Med 46:443–453
8. **Aoyagi S, Archer TK** 2008 Dynamics of coactivator recruitment and chromatin modifications during nuclear receptor mediated transcription. Mol Cell Endocrinol 280:1–5
9. **McEwen BS** 2010 Stress, sex, and neural adaptation to a changing environment: mechanisms of neuronal remodeling. Ann NY Acad Sci 1204(Suppl):E38–E59
10. **Datson NA, Morsink MC, Meijer OC, de Kloet ER** 2008 Central corticosteroid actions: search for gene targets. Eur J Pharmacol 583: 272–289
11. **Datson NA, Polman JA, de Jonge RT, van Boheemen PT, van Maanen EM, Welten J, McEwen BS, Meiland HC, Meijer OC** 2011 Specific regulatory motifs predict glucocorticoid responsiveness of hippocampal gene expression. Endocrinology 152:3749–3757
12. **Datson NA, Speksnijder N, Mayer JL, Steenbergen PJ, Korobko O, Goeman J, de Kloet ER, Joëls M, Lucassen PJ** 2012 The transcriptional response to chronic stress and glucocorticoid receptor blockade in the hippocampal dentate gyrus. Hippocampus 22:359–371
13. **Datson NA, van der Perk J, de Kloet ER, Vreugdenhil E** 2001 Identification of corticosteroid-responsive genes in rat hippocampus using serial analysis of gene expression. Eur J Neurosci 14:675–689
14. **Morsink MC, Steenbergen PJ, Vos JB, Karst H, Joëls M, De Kloet ER, Datson NA** 2006 Acute activation of hippocampal glucocorticoid receptors results in different waves of gene expression throughout time. J Neuroendocrinol 18:239–252
15. **Denver RJ, Ouellet L, Furling D, Kobayashi A, Fujii-Kuriyama Y, Puymirat J** 1999 Basic transcription element-binding protein (BTEB) is a thyroid hormone-regulated gene in the developing central nervous system. Evidence for a role in neurite outgrowth. J Biol Chem 274:23128–23134
16. **Denver RJ, Williamson KE** 2009 Identification of a thyroid hormone response element in the mouse Kruppel-like factor 9 gene to explain its postnatal expression in the brain. Endocrinology 150:3935–3943
17. **Imataka H, Nakayama K, Yasumoto K, Mizuno A, Fujii-Kuriyama Y, Hayami M** 1994 Cell-specific translational control of transcription factor BTEB expression. The role of an upstream AUG in the 5′-untranslated region. J Biol Chem 269:20668–20673
18. **Imataka H, Sogawa K, Yasumoto K, Kikuchi Y, Sasano K, Kobayashi A, Hayami M, Fujii-Kuriyama Y** 1992 Two regulatory proteins that bind to the basic transcription element (BTE), a GC box sequence in the promoter region of the rat P-4501A1 gene. EMBO J 11:3663–3671
19. **Morita M, Kobayashi A, Yamashita T, Shimanuki T, Nakajima O, Takahashi S, Ikegami S, Inokuchi K, Yamashita K, Yamamoto M, Fujii-Kuriyama Y** 2003 Functional analysis of basic transcription element binding protein by gene targeting technology. Mol Cell Biol 23:2489–2500
20. **Scobie KN, Hall BJ, Wilke SA, Klemenhagen KC, Fujii-Kuriyama Y, Ghosh A, Hen R, Sahay A** 2009 Kruppel-like factor 9 is necessary for late-phase neuronal maturation in the developing dentate gyrus and during adult hippocampal neurogenesis. J Neurosci 29:9875–9887
21. **Dussault JH, Ruel J** 1987 Thyroid hormones and brain development. Annu Rev Physiol 49:321–334
22. **Cayrou C, Denver RJ, Puymirat J** 2002 Suppression of the basic transcription element-binding protein in brain neuronal cultures inhibits thyroid hormone-induced neurite branching. Endocrinology 143:2242–2249
23. **Bonett RM, Hu F, Bagamasbad P, Denver RJ** 2009 Stressor and glucocorticoid-dependent induction of the immediate early gene kruppel-like factor 9: implications for neural development and plasticity. Endocrinology 150:1757–1765
24. **Quadrilatero J, Hoffman-Goetz L** 2005 In vivo corticosterone administration at levels occurring with intense exercise does not induce intestinal lymphocyte apoptosis in mice. J Neuroimmunol 162:137–148
25. **Denver RJ** 1998 Hormonal correlates of environmentally induced metamorphosis in the Western spadefoot toad, *Scaphiopus hammondii*. Gen Comp Endocrinol 110:326–336
26. **Licht P, McCreery BR, Barnes R, Pang R** 1983 Seasonal and stress

related changes in plasma gonadotropins, sex steroids, and corticosterone in the bullfrog, *Rana catesbeiana*. Gen Comp Endocrinol 50:124–145
27. **Manzon RG, Denver RJ** 2004 Regulation of pituitary thyrotropin gene expression during *Xenopus* metamorphosis: negative feedback is functional throughout metamorphosis. J Endocrinol 182:273–285
28. **Ziera T, Irlbacher H, Fromm A, Latouche C, Krug SM, Fromm M, Jaisser F, Borden SA** 2009 Cnksr3 is a direct mineralocorticoid receptor target gene and plays a key role in the regulation of the epithelial sodium channel. FASEB J 23:3936–3946
29. **Morimoto BH, Koshland Jr DE** 1990 Induction and expression of long- and short-term neurosecretory potentiation in a neural cell line. Neuron 5:875–880
30. **Morimoto BH, Koshland Jr DE** 1990 Excitatory amino acid uptake and N-methyl-D-aspartate-mediated secretion in a neural cell line. Proc Natl Acad Sci USA 87:3518–3521
31. **Sagara Y, Dargusch R, Chambers D, Davis J, Schubert D, Maher P** 1998 Cellular mechanisms of resistance to chronic oxidative stress. Free Radic Biol Med 24:1375–1389
32. **Maher P, Davis JB** 1996 The role of monoamine metabolism in oxidative glutamate toxicity. J Neurosci 16:6394–6401
33. **Rozeboom AM, Akil H, Seasholtz AF** 2007 Mineralocorticoid receptor overexpression in forebrain decreases anxiety-like behavior and alters the stress response in mice. Proc Natl Acad Sci USA 104:4688–4693
34. **Samuels HH, Stanley F, Casanova J** 1979 Depletion of L-3,5,3′-triiodothyronine and L-thyroxine in euthyroid calf serum for use in cell culture studies of the action of thyroid hormone. Endocrinology 105:80–85
35. **Yao M, Schulkin J, Denver RJ** 2008 Evolutionarily conserved glucocorticoid regulation of corticotropin-releasing factor expression. Endocrinology 149:2352–2360
36. **Hoopfer ED, Huang L, Denver RJ** 2002 Basic transcription element binding protein is a thyroid hormone-regulated transcription factor expressed during metamorphosis in *Xenopus laevis*. Dev Growth Differ 44:365–381
37. **Blauwkamp TA, Chang MV, Cadigan KM** 2008 Novel TCF-binding sites specify transcriptional repression by Wnt signalling. EMBO J 27:1436–1446
38. **Denver RJ, Pavgi S, Shi YB** 1997 Thyroid hormone-dependent gene expression program for *Xenopus* neural development. J Biol Chem 272:8179–8188
39. **de Kloet ER, Reul JM, Sutanto W** 1990 Corticosteroids and the brain. J Steroid Biochem Mol Biol 37:387–394
40. **Veldhuis HD, Van Koppen C, Van Ittersum M, De Kloet ER** 1982 Specificity of the adrenal steroid receptor system in rat hippocampus. Endocrinology 110:2044–2051
41. **Arriza JL, Simerly RB, Swanson LW, Evans RM** 1988 The neuronal mineralocorticoid receptor as a mediator of glucocorticoid response. Neuron 1:887–900
42. **Furlow JD, Kanamori A** 2002 The transcription factor basic transcription element-binding protein 1 is a direct thyroid hormone response gene in the frog *Xenopus laevis*. Endocrinology 143:3295–3305
43. **Lin Y, Bloodgood BL, Hauser JL, Lapan AD, Koon AC, Kim TK, Hu LS, Malik AN, Greenberg ME** 2008 Activity-dependent regulation of inhibitory synapse development by Npas4. Nature 455:1198–1204
44. **So AY, Cooper SB, Feldman BJ, Manuchehri M, Yamamoto KR** 2008 Conservation analysis predicts in vivo occupancy of glucocorticoid receptor-binding sequences at glucocorticoid-induced genes. Proc Natl Acad Sci USA 105:5745–5749
45. **Luebben WR, Sharma N, Nyborg JK** 2010 Nucleosome eviction and activated transcription require p300 acetylation of histone H3 lysine 14. Proc Natl Acad Sci USA 107:19254–19259
46. **Toni N, Laplagne DA, Zhao C, Lombardi G, Ribak CE, Gage FH, Schinder AF** 2008 Neurons born in the adult dentate gyrus form functional synapses with target cells. Nat Neurosci 11:901–907
47. **Leuner B, Gould E** 2010 Structural plasticity and hippocampal function. Annu Rev Psychol 61:111–140:C111–C113